

Proximity Effects and Quantum Dissipation in the Chains of $\text{YBa}_2\text{Cu}_3\text{O}_{6+x}$

Dirk K. Morr and Alexander V. Balatsky

Theoretical Division, MS B262, Los Alamos National Laboratory, Los Alamos, NM 87545
(November 13, 2018)

We argue that the results of recent scanning tunneling microscopy, angle-resolved photoemission and infrared spectroscopy experiments on the CuO chains of $\text{YBa}_2\text{Cu}_3\text{O}_{6+x}$ are consistently explained within a proximity model by the interplay of a *coherent* chain-plane and an *incoherent* interchain coupling. We show that the CuO_2 planes act as an ohmic heat bath for the electronic degrees of freedom in the chains which induces a substantial quantum dissipation. Below the planar T_c , charge excitations in the chains acquire a *universal* superconducting gap whose phase and magnitude are *momentum* dependent. We predict that the magnitude of this gap varies non-monotonically with the hole concentration in the chains.

PACS numbers: 74.50.+r, 74.25.Jb, 74.25.-q

Little is known about the coupling of the CuO_2 planes and CuO chains in $\text{YBa}_2\text{Cu}_3\text{O}_{6+x}$ (YBCO) and how the onset of planar superconductivity affects the electronic degrees of freedom in the chains. The observation of a superfluid component in the chains below the planar T_c in infrared spectroscopy (IS) experiments by Basov *et al.* [1] suggests that the chains undergo a proximity-induced superconducting (PSC) transition. This scenario is consistent with recent scanning tunneling microscopy (STM) experiments [2,3] which reported a large gap $\sim 15 - 25$ meV in the chain density of states (CDOS) below T_c . Additional information comes from angle-resolved photoemission (ARPES) experiments which observed a sharp peak as well as a large incoherent "hump" in the chain spectral function, A_c [4].

In this Letter we show that the above-cited results of IS, STM and ARPES experiments are consistently explained within a proximity model by the interplay of a *coherent* chain-plane (CP) and an *incoherent* interchain (IC) coupling [5]. We demonstrate that the coherent/incoherent nature of these couplings causes the CuO_2 planes to be an ohmic heat bath for the electronic degrees of freedom in the chains. As a result, the chains exhibit a substantial quantum dissipation, similar to the case of a two-level system coupled to set of harmonic oscillators [6]. With the onset of planar superconductivity a frequency gap opens in the dissipative heat bath, and a Fermi-gas like peak appears in the chain spectral function. Simultaneously, charge excitations in the chains acquire a *universal* superconducting (SC) gap whose phase and magnitude are *momentum* dependent. We predict that the magnitude of this gap varies non-monotonically with the hole concentration in the chains. Since the intrabilayer coupling in YBCO was shown to be coherent [7], our results immediately imply that the c-axis transport in YBCO, a topic extensively discussed over the last few years [8], is necessarily dominated by coherent electronic hopping.

For the calculation of the CDOS and spectral function, measured in surface sensitive ARPES and STM experiments, we consider an infinite array of CuO -chains

which is aligned along the x-axis and coupled to a single CuO_2 -plane via a hopping term t_\perp [9]. We neglect the second CuO_2 -plane in the bilayer unit cell since the planes are only weakly coupled [7]. We assume that the superconducting pairing interaction resides solely in the plane, and describe the planar electrons by a mean-field BCS-hamiltonian. The hamiltonian for the chain-plane system is thus given by

$$\mathcal{H} = \sum_{\mathbf{k}, \sigma} \epsilon_{\mathbf{k}} c_{\mathbf{k}, \sigma}^\dagger c_{\mathbf{k}, \sigma} + \sum_{\mathbf{k}} \left(\Delta_{\mathbf{k}} c_{\mathbf{k}, \uparrow}^\dagger c_{\mathbf{k}, \downarrow}^\dagger + h.c. \right) + \sum_{k, \sigma} \zeta_{\mathbf{k}} d_{k, \sigma}^\dagger d_{k, \sigma} - t_\perp \sum_{k, \sigma} \left(c_{k, \sigma}^\dagger d_{k, \sigma} + h.c. \right) \quad (1)$$

where $c_{\mathbf{k}}^\dagger, d_{\mathbf{k}}^\dagger$ are the fermionic creation operators in the plane and chain, respectively. The tight-binding dispersions for the plane and chain electrons, $\epsilon_{\mathbf{k}}$ and $\zeta_{\mathbf{k}}$, are given by

$$\epsilon_{\mathbf{k}} = -2t_p \left(\cos(k_x) + \cos(k_y) \right) - 4t'_p \cos(k_x) \cos(k_y) - \mu_p, \quad \zeta_{\mathbf{k}} = -2t_c \cos(k_x) - \mu_c. \quad (2)$$

Here, $t_p, t'_p(t_c)$ are the planar (chain) hopping elements between nearest and next-nearest neighbors, respectively, and $\mu_p(\mu_c)$ is the planar (chain) chemical potential. The planar SC gap is given by $\Delta_{\mathbf{k}} = \Delta_{SC} (\cos(k_x) - \cos(k_y))/2$.

An effective action for the chain electrons, S_c , is obtained by integrating out the planar electronic degrees of freedom. One obtains

$$\mathcal{S} = \sum_{\omega_n, l, m} \int dk_x \hat{d}_l^\dagger \hat{G}_c^{-1}(\omega_n, k_x, l, m) \hat{d}_m, \quad (3)$$

where l, m are chain indices, and

$$\hat{d}_l^\dagger = (d_{l, \uparrow}^*(k_x, \omega_n), d_{l, \downarrow}(-k_x, -\omega_n)) . \quad (4)$$

For the matrix \hat{G}_c^{-1} one has

$$\hat{G}_c^{-1} = \begin{pmatrix} G_0^{-1}(k_x, \omega_n) & F_0^{-1}(k_x, \omega_n) \\ F_0^{-1}(k_x, \omega_n) & -G_0^{-1}(-k_x, -\omega_n) \end{pmatrix}, \quad (5)$$

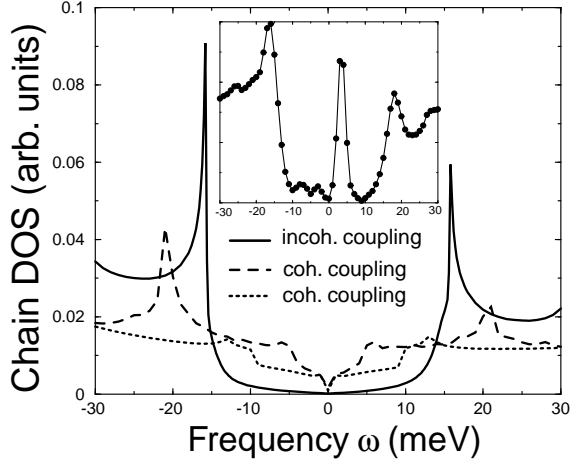


FIG. 1. Chain DOS in the SC state for $t_{\perp} = 0.4t_p$ and $\Delta_{SC} = 40$ meV. Solid line: incoherent IC coupling. Dashed line: coherent IC coupling. Dotted line: coherent IC coupling with $\Delta_{SC} = 100$ meV. Inset: Experimental data taken from Ref. [3].

where

$$G_0^{-1} = (i\omega_n - \zeta_{\mathbf{k}}) \delta_{l,m} - t_{\perp}^2 N^{-1} \sum_{k_y} \frac{i\omega_n + \epsilon_{\mathbf{k}}}{(i\omega_n)^2 - (\epsilon_{\mathbf{k}})^2 - \Delta_k^2} e^{ik_y(l-m)}; \\ F_0^{-1} = -t_{\perp}^2 N^{-1} \sum_{k_y} \frac{\Delta_k}{(i\omega_n)^2 - (\epsilon_{\mathbf{k}})^2 - \Delta_k^2} e^{ik_y(l-m)}. \quad (6)$$

The chain Greens function for coherent IC coupling is straightforwardly computed from Eqs.(3) and (5). In contrast, in the case of incoherent IC coupling where the coherent correlations between the chains are destroyed, one evaluates Eq.(3) using the ansatz

$$\hat{G}_c^{-1}(k_x, l, m, \omega_n) = \hat{G}_c^{-1}(k_x, \omega_n) \delta_{l,m}. \quad (7)$$

Our theoretical results for the CDOS and spectral function presented in the following are obtained by using a set of band parameters, $t_p = 300$ meV, $t'_p/t_p = -0.4$, $\mu_p/t_p = -1.18$, extracted from ARPES experiments on YBCO [4] and a planar SC gap, $\Delta_{SC} \approx 35 - 40$ meV, representative of that in slightly underdoped YBCO compounds [10]. The chain Fermi momentum, $k_F^c \approx 0.25\pi$, was extracted from INS [11] and STM experiments [2], and yields $\mu_c/t_c = -1.41$, corresponding to a hole concentration of $x \approx 50\%$ in the chains.

In Fig. 1 we present our theoretical results for the chain DOS, $N(\omega) = N^{-1} \sum_{\mathbf{k}} A_c(k, \omega)$ [12], together with the experimental results of Ref. [3]. The possible impurity origin of the peak in the experimental CDOS at $\omega \approx 3$ meV [13] is beyond the scope of the present letter and will be addressed in a future study. Our theoretical result for the chain DOS for incoherent IC coupling (solid line) are in good agreement with the experimentally measured

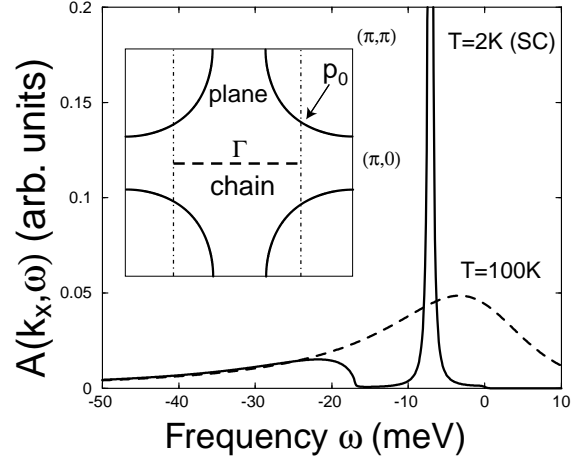


FIG. 2. Frequency dependence of A_c for incoherent IC coupling at the chain Fermi momentum, $k_F^c = 0.25\pi$, in the normal (dashed line) and superconducting state (solid line).

magnitude of the chain gap, $\Delta_c^{exp} \approx 17$ meV, as well as the observed particle-hole asymmetry of the CDOS. The simultaneous appearance of an anomalous chain Greens function, F_0 , in Eq.(5) demonstrates that the induced gap is related to the onset of superconductivity in the chains. In contrast, the CDOS for coherent IC coupling (dashed line) and the same set of parameters does not only possess a much smaller gap [14], but its overall frequency dependence is also inconsistent with the experimental data. We explored various sets of band parameters and did not find an improved agreement with the experimental data, even for an unphysically large superconducting gap of $\Delta_{SC} = 100$ meV (dotted line in Fig. 1). Moreover, for incoherent CP coupling (and thus incoherent IC coupling), no gap is induced in the CDOS and $F_0^{-1} \equiv 0$ in Eq.(5); hence no superconducting correlations are present in the chains, in disagreement with the results of IS experiments [1]. We thus conclude that the experimental STM and IS data provide strong evidence for an incoherent interchain and coherent chain-plane coupling in YBCO.

Before we can address the physical origin of the different CDOS for coherent and incoherent IC coupling, it is necessary to study the spectral function, $A_c(k, \omega)$, for incoherent IC coupling, in more detail. In Fig. 2 we present our numerical results for A_c at k_F^c [12]; for comparison with ARPES measurements we have multiplied A_c with the Fermi distribution function $n_F = (\exp(\omega/k_B T) + 1)^{-1}$, which shifts the peak in A_c to lower energies. In the normal state (dashed line) the spectral function exhibits a broad peak, indicating a strong quasiparticle damping. The source of the quasiparticle dissipation is best understood by analytically evaluating the integrals on the r.h.s. of Eq.(6). One obtains for the retarded chain Greens function at momentum k_x

$$G_c^R(k_x, \omega) = \frac{1}{\omega - \zeta_k + i\alpha}, \quad (8)$$

where $\alpha = t_\perp^2/\bar{v}$, $\bar{v} = (\partial\epsilon_{\mathbf{k}}/\partial k_y)|_{\mathbf{p}_0}$, and \mathbf{p}_0 is a momentum on the planar Fermi surface (FS) with $p_0^x = k_x$ (see inset of Fig. 2). Due to the coupling, t_\perp , the chain electrons can decay into a continuum of planar states perpendicular to the chain direction. The planes thus represent a dissipative environment which gives rise to a frequency independent quasiparticle damping, α . This form of dissipation is analogous to the ‘‘ohmic case’’ discussed by Leggett *et al.* [6] for a two-level system coupled to a set of one-dimensional harmonic oscillators, which constitute a similar dissipative ‘‘heat bath’’. Thus, α does *not* arise from a Coulomb-type interaction, but from the different dimensionality of the chain and plane system.

With the onset of superconductivity, the planar heat bath acquires a gap and the frequency dependence of A_c (solid line in Fig. 2) changes dramatically. At low frequencies, the damping of the chain electrons is strongly reduced and a Fermi-gas-like low-frequency quasiparticle peak (LFQP) appears. The suppression of the quasiparticle damping arises from a kinematic constraint since a chain electron can only decay into the continuum of planar states if its frequency exceeds the necessary energy, $\bar{\Delta}(k_x) = |\Delta(\mathbf{p}_0)|$, to break a Cooper-pair. Hence, one recovers a substantial quasiparticle damping only for $\omega > \bar{\Delta}(k_x)$. Moreover, the LFQP is shifted downward in energy from the position of the broad peak at $\omega = 0$ in the normal state (cf. solid line), indicating the presence of a gap for electronic excitations in the chains. This gap arises from a virtual hopping of a chain electron into the planar continuum states, a process which lowers the electron’s ground state energy; hence, one expects the gap to be of order t_\perp^2/v_F . Moreover, an analysis of F_0 , Eq.(6), shows that the phase of the induced gap is *momentum* dependent and changes at k_n , where $\mathbf{K}_{node} = (k_n, k_n)$ is the momentum of the planar SC nodes. The separation of the LFQP and the incoherent background by a dip in Fig. 2 is reminiscent of planar ARPES data [15] where a decrease of the fermionic damping in the SC state due to the opening of a spin gap gives also rise to a ‘‘peak-dip-hump’’ structure in the spectral function.

In order to better understand the momentum dependence of A_c below T_c , it is necessary to analytically study the retarded chain Greens function, G_c^R , in Eq.(6). One obtains

$$G_c^R = B(\omega, k_x)^{-1} \left[\omega + \zeta_k + \frac{\alpha\omega}{\sqrt{\bar{\Delta}^2 - \omega^2}} \right], \quad (9)$$

where

$$B(\omega, k_x) = \omega^2 \left(1 + \frac{\alpha}{\sqrt{\bar{\Delta}^2 - \omega^2}} \right)^2 - (\zeta_k)^2 - \left(\frac{\alpha\bar{\Delta}}{\sqrt{\bar{\Delta}^2 - \omega^2}} \right)^2, \quad (10)$$

and $\omega = \omega + i\delta$. The dispersion, χ_k , of the LFQP is

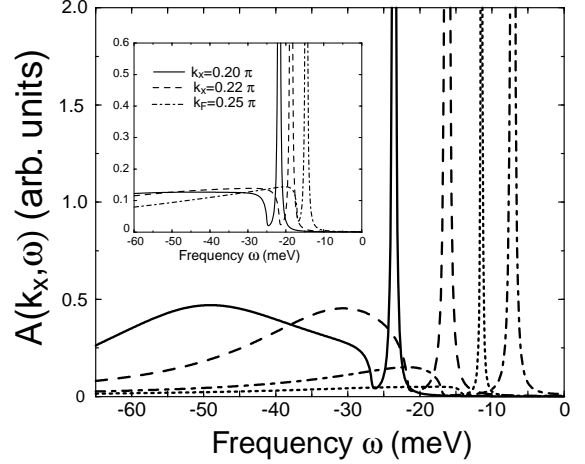


FIG. 3. A_c as a function of frequency for $t_\perp = 0.18t$, $\mu_c = -1.41t_c$ and four momenta: $k_x = 0.19\pi$ (solid line), $k_x = 0.22\pi$ (dashed line), $k_F^c = 0.25\pi$ (dashed-dotted line), and $k_x = 0.27\pi$ (dotted line). Inset: A_c for $t_\perp = 0.40t_p$ and three momenta.

determined by $\text{Re} B(\omega = \chi_k) = 0$. In the limit $\alpha^2 + \zeta_k^2 \ll \bar{\Delta}^2$, i.e., close to the chain Fermi points, one has

$$\chi_k = \pm \sqrt{\alpha + \zeta_k^2}, \quad (11)$$

where α is the *universal* SC chain gap, which is independent of the planar gap, Δ_{SC} . In the opposite limit, $\alpha^2 + \zeta_k^2 \gg \bar{\Delta}^2$, one obtains

$$\chi_k = \pm \bar{\Delta} \left[1 - \frac{2\alpha^2 \bar{\Delta}^2}{(\alpha^2 + \zeta_k^2)^2} \right], \quad (12)$$

and the LFQP is thus confined to frequencies $|\omega| < |\bar{\Delta}|$ for all k_x . In addition, one finds a high-frequency quasiparticle peak (HFQP) whose dispersion is given by $\phi_k = \pm \sqrt{\zeta_k^2 + \alpha^2}$. Since $\phi_k > |\bar{\Delta}|$, the HFQP is overdamped with

$$A_c(k, \omega = \phi_k) = \sqrt{\phi_k^2 - \bar{\Delta}^2} \frac{\phi_k + \zeta_k}{\alpha\phi_k^2} \sim \alpha^{-1}. \quad (13)$$

In the limit $\zeta_k \gg \max\{\bar{\Delta}, \alpha\}$, the HFQP follows the dispersion of the free chain electrons, $\phi_k = \zeta_k$, with a *momentum independent* intensity, $A_c = \alpha^{-1}$.

In Fig. 3 we present our numerical results for A_c in the SC state for several momenta around k_F^c . For momenta much below k_F^c ($k_x = 0.19\pi$, solid line; $k_x = 0.22\pi$, dashed line) A_c possesses a HFQP and a LFQP, which both move to higher energies as k_x approaches k_F^c . The dispersion of the LFQP is much weaker than that of the HFQP, since the LFQP is located close to $\bar{\Delta}(k_x)$ which changes only weakly with momentum while the HFQP’s dispersion is given by ζ_k . Note the momentum independence of the HFQP’s intensity. At the Fermi momentum, $k_F^c = 0.25\pi$, the HFQP has disappeared and only a

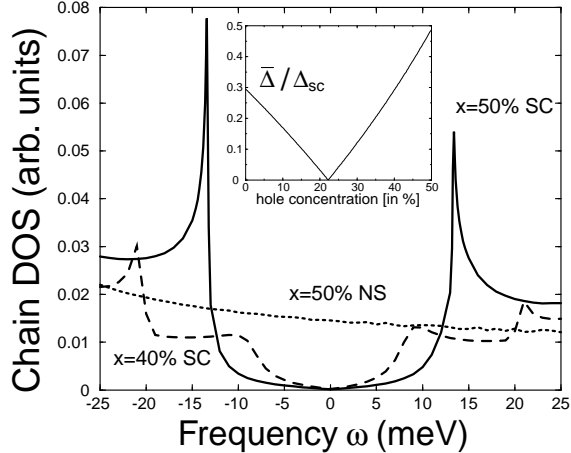


FIG. 4. DOS for $t_{\perp} = 0.4t_p$, and two different hole concentration, x : (a) $x = 50\%$, SC state (solid line) and normal state (dotted line), (a) $x = 40\%$ SC state (dashed line). Inset: $\bar{\Delta}(k_F^c)/\Delta_{SC}$ as a function of hole concentration in the chains.

broad incoherent background remains with a maximum close to its onset frequency $\bar{\Delta} \approx -17$ meV. For momenta above k_F^c ($k_x = 0.27\pi$, dashed-dotted line) the LFQP shifts again to lower energies, while its intensity and that of the incoherent background decreases rapidly. An increased CP coupling ($t_{\perp} = 0.4t_p$, see inset of Fig. 3) leaves A_c qualitatively unchanged, albeit with a much broader HFQP. The momentum and frequency dependence of A_c shown in Fig. 3 is in qualitative agreement with recent ARPES experiments by Schabel *et al.* [4] in the SC state of $\text{YBa}_2\text{Cu}_3\text{O}_{6.95}$. They also report a broad dispersing peak for momenta $k_x \ll k_F^c$, while for $k_x \approx k_F^c$, A_c exhibits a hump and a sharper quasi-particle peak (cf. Fig. 7d in Ref. [4]).

The gap induced in the CDOS for incoherent IC coupling varies strongly with the hole concentration, x , in the chains, as shown in Fig. 4. For $t_{\perp} = 0.4t_p$, one finds $\alpha > \bar{\Delta}(k_F^c)$ and hence the frequency of the gap edges in the CDOS is determined by $\bar{\Delta}(k_F^c)$ (cf. Eq(12)). Since $\bar{\Delta}(k_F^c)$ decreases as the hole concentration is reduced from $x = 50\%$ to $x = 40\%$ (see inset of Fig. 4), the magnitude of the induced gap also decreases, in agreement with our results in Fig. 4. The gap in the CDOS is the smallest for $x = 22\%$, since here $k_F^c = k_n$ and $\bar{\Delta}(k_F^c) = 0$. We thus predict that the gap in the CDOS varies non-monotonically with x : as x is decreased from $x = 50\%$ the induced gap first decreases, exhibits a minimum at $x = 22\%$ and then increases again for even smaller hole concentrations. Moreover, for small frequencies we find $N(\omega) \sim \omega$ which is a direct consequence of the linear momentum dependence of Δ_k in the vicinity of the nodes. In contrast, the chain DOS in the normal state (dashed line) is only weakly frequency and doping dependent.

The origin of the qualitatively different CDOS for coherent and incoherent IC coupling is twofold. First, for

coherent IC coupling, the chain states are described by a two-dimensional momentum, \mathbf{k} , and the dimensionality of the *coherent* chain array and the CuO_2 planes is the same. Thus, the CuO_2 planes do not constitute a dissipative environment for the electronic degrees of freedom in the chains. Second, the changes which occur in the CDOS for a given frequency, ω , upon entering the SC state arise from those electronic states which can reduce their ground state energy by a virtual hopping process into the planes. It follows from Eqs.(5) and (6) that in the case of coherent IC coupling these states must satisfy $t_{\perp}^2 \gg \omega^2 - \epsilon_k^2 - \Delta_k^2$. Simple phase space counting shows that the number of states which undergo a shift in the ground state energy is much smaller for coherent than for incoherent IC coupling. As a result, the CDOS for incoherent IC coupling exhibits a much larger SC gap than that for coherent IC coupling.

Two explanations for the absence of a coherent IC coupling in YBCO are possible. First, STM experiments have provided evidence for inhomogeneous doping in the chains. The resulting distribution of Fermi momenta likely prevents the coherent coupling between momenta in the vicinity of k_F^c , and thus renders the coupling incoherent. Second, a series of experimental probes have reported charge and spin inhomogeneities (stripes) in the CuO_2 planes which are aligned parallel to the chains [16]. Since planar electrons are likely scattered by these inhomogeneities, a coherent coupling only exists between those chains which can be connected by an electron path that is not intersected by a stripe. This scenario can be tested in the underdoped YBCO compounds where the stripe-stripe distance increases and coherent IC coupling between an increasing number of chains is expected.

Recently, there has been an extensive discussion on the relative strength of incoherent versus coherent hopping of carriers between the planes [8]. Since the CP hopping is a part of the hopping process between the bilayers in YBCO, our results support the notion that coherent hopping is a crucial part of the communication of electrons between the planes. Though the CP hopping, t_{\perp} , in the bulk is likely somewhat reduced from the value extracted above (the distance between the surface chain layer and the next CuO_2 layer is smaller than the corresponding separation in the bulk [13]) we expect it to remain coherent.

Finally, the phase of the induced SC gap as well as its non-monotonic doping dependence, Fig. 4, are salient features of the PSC state which distinguish it from other possible ground states, e.g., a charge-density-wave. We thus propose phase-sensitive Josephson tunneling or Josephson STM experiments as a crucial test for our above scenario.

In summary, we propose a scenario in which the results of recent IS, STM and ARPES experiments on the chains of YBCO can consistently be explained by the interplay of a coherent chain-plane coupling and an incoherent interchain coupling. We show that the CuO_2 planes act as a dissipative environment for the electronic

degrees of freedom in the chains and induce a substantial quantum dissipation. We find that the chains exhibit superconducting correlations and a *universal* gap below T_c , and predict that the magnitude of this gap varies non-monotonically with the hole concentration in the chains.

We would like to thank P.W. Anderson, W.A. Atkinson, A. Chubukov, J.C. Davis (JCD), A. de Lozanne (AdL), J. Schmalian, and J. Zaanen for stimulating discussions, and JCD and AdL for providing us with their experimental data prior to publication. This work has been supported by the Department of Energy at Los Alamos.

-
- [1] D.N. Basov *et al.*, Phys. Rev. Lett. **74**, 598 (1995).
 - [2] H.L. Edwards *et al.*, Phys. Rev. Lett. **73**, 1154 (1994); H.L. Edwards *et al.*, Phys. Rev. Lett. **75**, 1387 (1995).
 - [3] A. de Lozanne *et al.*, preprint.
 - [4] M.C. Schabel *et al.*, Phys. Rev. B **57**, 6090 (1998).
 - [5] Since no direct IC coupling is possible in YBCO, any IC coupling is necessarily mediated by the CuO₂ planes.
 - [6] A.J. Leggett *et al.*, Rev. Mod. Phys. **59**, 1 (1987).
 - [7] S.M Hayden *et al.*, Phys. Rev. B **54**, R6905 (1996).
 - [8] A.J. Leggett, Phys. Rev. Lett. **83**, 392 (1999); P.W. Anderson, Science **279**, 1196 (1998); K. Wonkee and J.P. Carbotte, Phys. Rev. B **61**, R11886 (2000).
 - [9] The surface layer in cleaved YBCO is the chain layer, followed by a CuO₂ plane.
 - [10] I. Maggio-Aprile *et al.*, J. Low Temp. Phys. **105**, 1129 (1996).
 - [11] H. A. Mook *et al.*, Phys. Rev. Lett. **77**, 370 (1996).
 - [12] Our numerical results for $A_c = -2\text{Im}G_c^R/\pi$ are obtained from Eq.(6) via the analytical continuation $i\omega_n \rightarrow \omega + i\delta$ with $\delta = 0.1$ meV.
 - [13] A. de Lozanne, private communication.
 - [14] W.A. Atkinson, Ph.D-thesis, McMaster University (1995), unpublished.
 - [15] A.V. Chubukov and D.K. Morr, Phys. Rev. Lett. **81**, 4716 (1998).
 - [16] H.A. Mook *et al.*, Nature **404**, 729 (2000).